



City Research Online

City, University of London Institutional Repository

Citation: Mergos, P.E. & Kawashima, K. (2005). Rocking isolation of a typical bridge pier on spread foundation. *Journal of Earthquake Engineering*, 9(SPEC. ISS. 2), pp. 395-414. doi: 10.1142/S1363246905002456

This is the unspecified version of the paper.

This version of the publication may differ from the final published version.

Permanent repository link: <https://openaccess.city.ac.uk/id/eprint/3635/>

Link to published version: <https://doi.org/10.1142/S1363246905002456>

Copyright: City Research Online aims to make research outputs of City, University of London available to a wider audience. Copyright and Moral Rights remain with the author(s) and/or copyright holders. URLs from City Research Online may be freely distributed and linked to.

Reuse: Copies of full items can be used for personal research or study, educational, or not-for-profit purposes without prior permission or charge. Provided that the authors, title and full bibliographic details are credited, a hyperlink and/or URL is given for the original metadata page and the content is not changed in any way.

City Research Online:

<http://openaccess.city.ac.uk/>

publications@city.ac.uk

ROCKING ISOLATION OF A TYPICAL BRIDGE PIER ON SPREAD FOUNDATION

PANAGIOTIS ELIA MERGOS

*European School for Advanced Studies in Reduction of Seismic Risk (Rose School)
Via Ferrata, 27100 Pavia, Italy*

KAZUHIKO KAWASHIMA

*Department of Civil Engineering, Tokyo Institute of Technology
O-Okayama, Meguro, 152-8552 Tokyo, Japan*

It has been observed that after some earthquakes a number of structures resting on spread footings responded to seismic excitation by rocking on their foundation and in some cases this enabled them to avoid failure. Through application to a standard bridge supported by direct foundations, this paper discusses the major differences in response when foundation uplift is taken into consideration. Special focus is given on the modifications of rocking response under biaxial and tri-axial excitation with respect to uniaxial excitation. It is found that inelastic rocking has a significant isolation effect. It is also shown that this effect increases under biaxial excitation while it is less sensitive to the vertical component of the earthquake. Finally, parametric analyses show that the isolation effect of foundation rocking increases as the size of the footing and the yield strength of the underlying soil decreases.

Keywords: Bridge; pier; rocking; uplift; isolation; biaxial excitation; tri-axial excitation

1. Introduction

Spread foundations are widely used to support bridge piers where the soil condition is stable. They are designed so that seismic performance for sliding, settlement and overturning is assured. Since overturning is generally critical in the design of direct foundations, it is important to clarify the safety of direct foundations against overturning.

Dynamic rocking response of structures has been in the center of scientific research over the last four decades ([Housner, 1963], [Clough *et al.*, 1977], [Priestley *et al.*, 1978], [Psycharis, 1982]). As investigated by Kawashima *et al.*, foundations do not overturn even if they are subjected to ground motions with peak accelerations larger than the static accelerations used in the traditional static analysis [Kawashima *et al.*, 1989, 1991, 1994, 2003]. This effect was taken into account in seismic design of Honshu-Shikoku Bridges, including Akashi Straight Bridge and Kurushima straight Bridge. Ciampoli and Pinto showed the importance of rocking response and bridge response interaction [Ciampoli *et*

al., 1995]. Priestley *et al.* presented the contribution of rocking response of a footing to the total deck displacement [Priestley *et al.*, 1996]. Finally, Cremer *et al.* presented a macro-element which included foundation uplift in modelling nonlinear dynamic behaviour of strip foundations [Cremer *et al.*, 2001].

This paper presents an analysis of a standard bridge supported by direct foundations and shows an isolation effect of inelastic rocking of the foundations. Modifications in rocking response under biaxial and tri-axial excitation with respect to uniaxial excitation are reported. Finally, parametric analyses show the influence of the yield strength of the underlying soil and the size of the footing on rocking isolation.

2. Bridge Analyzed

The bridge which is analyzed here is presented in Fig. 1. It is a 200m long, 5 span continuous bridge supported by 2 abutments and 4 reinforced concrete columns. The abutments and columns rest on 6 direct foundations. The superstructure consists of a plate girder deck.

The foundations are constructed in a sandy layer with their bottoms resting on gravels having N-value of the standard penetration test over 50. Subgrade elastic modulus, k_{sv} (kN/m^3), is 10^5 and yield strength of the underlying soil, σ_y , is 6MPa. The fundamental natural period of this ground is less than 0.2sec. This site is regarded as a stiff site (Group I Ground) according to the Japanese highway bridge design code.

Since the bridge and the soil conditions are uniform along the bridge axis, a structural system consisting of a column, a foundation and a tributary deck is analyzed here. The seismic response in the longitudinal direction is analyzed because it is the major concern in seismic design.

Fig. 2 represents the geometry of a typical pier of the bridge as well as the reinforcements at the critical cross section at the base of the pier.

In the design of the footing traditional static seismic analysis has been used. The static moment capacity of the square footing against overturning is:

$$M_{over}^{cap} = \frac{N \cdot L}{2} = 61.5 \text{ MNm} \quad (1)$$

where, N is the static axial load coming from the deck, the pier and the footing and L is the length of the footing.

After performing a moment- curvature analysis of the critical cross section of the pier in both horizontal directions, it is found that the nominal yield moments are equal to 49.6MNm and 109.6MNm in the longitudinal and the transversal direction of the bridge respectively.

3. Analytical Model and Ground Motions

The foundation, the column and a part of the deck are idealized by a discrete analytical model as shown in Fig. 3. The column is idealized by the Takeda degrading hysteretic model in the plastic hinge and linear beam elements with the stiffness corresponding to flexural yielding elsewhere. The foundation and the deck are idealized to be rigid and their masses are lumped at their centers of gravity.

Overburden soil was assumed to oscillate with the footing, so the weight of the overburden soil was added to the weight of the footing. Side friction of the overburden soil (overburden soil vs. soils beside the overburden soil) and the footing (footing vs. side soil) was disregarded.

Assuming that the subgrade reaction of the soil (gravels) per unit area, k_{sv} , is constant at the entire response displacement range of the footing, the rotational stiffness of the foundation when we neglect uplifting of the footing from the ground may be obtained in each direction as:

$$K_{rot} = \int_{-L/2}^{L/2} (k_{sv} \cdot x^2 \cdot B) dx = \frac{k_{sv} \cdot B \cdot L^3}{12} \quad (2)$$

where L and B are the length and the width of the rectangular footing respectively.

When separation of the footing from the underlaid ground is taken into account, the rotational stiffness of the foundation in each direction is a nonlinear function of the respective rotation. Furthermore, the stiffnesses of the footing in the two horizontal directions are not uncoupled anymore. This is because foundation uplift in one direction reduces the stiffness of the footing in the other direction. Consequently, a three-dimensional Winkler foundation model is used with the individual soil springs having nonlinear restoring force characteristics. In compression, stiffness and yield strength of an individual soil spring are the products of its corresponding area times k_{sv} and σ_y respectively. In separation, soil springs are assumed to have zero stiffness.

Near-field ground motion recorded at JMA Kobe Observatory in the 1995 Kobe, Japan earthquake is used as an input ground motion. The NS component is applied in the longitudinal direction of the bridge and the EW component in the transversal.

In the analysis, the Newmark constant average acceleration method (implicit method) is used. As the footing uplifts from the ground a sudden change in spring stiffness occurs. This change results in high unbalanced forces in the equilibrium of equations of motion. A residual force at the end of each time step is added to the incremental external force at the next time step in order to avoid numerical instability. The stiffness of an individual spring and the time interval of numerical integration Δt are factors influencing significantly the results in the idealization of poundings of the footing with the ground.

By comparing a very sensitive response parameter, like the vertical acceleration at a corner of the footing, it is found in this example that a mesh composed by 361 springs (distance between the springs is 0.5m) combined with a time interval of numerical integration $\Delta t=0.0025\text{sec}$ provides accurate results. It is worth noting that the peak vertical accelerations obtained by using $\Delta t=0.01\text{sec}$ and the same mesh of Winkler

springs are almost two times the respective responses derived by the smaller Δt . The solution converges much faster for other less sensitive response parameters like the velocities and the displacements of the structure.

It is known that sliding and uplift of a rocking body develops a complex interaction between sliding, rocking and jumping [Ishiyama, 1982]; however the sliding is restrained in the following analyses because sliding is not critical in this foundation.

Finally, radiational energy dissipation at the base of the footing when separation and contact with the underlying soil occur was disregarded due to the complexity of the problem. This needs further clarification in the future.

4. Response of the Bridge under Uniaxial Excitation

The deck displacement u in the longitudinal direction comes from the translation and rotation of the footing and the elastic and plastic flexure of the column as:

$$u = u_{ft} + \theta_f h_o + u_{pp} + u_{pf} \quad (3)$$

in which u_{ft} and θ_f are the translation and rotation of the footing, respectively, h_o is the distance from the bottom of the pier to the center of the deck, u_{pp} is the deck displacement resulted from the plastic rotation of the column in the plastic hinge, and u_{pf} is the deck displacement resulted from the elastic flexural deformation of the column. Among those quantities, u_{ft} is restrained in this analysis.

The seismic response of the bridge subjected to the NS component of JMA Kobe observatory record in the longitudinal direction is presented in Fig. 4. When separation of the footing from the ground is not taken into account, it is found that the peak deck displacement is 0.32m. The respective displacement of the deck due to foundation rocking is only 0.02m. This is only 4.7% of the total deck displacement. The maximum deck displacement due to plastic behaviour of the pier is 0.22m. On the other hand, when separation of the footing from the ground is taken into consideration the peak total displacement is 0.27m and the respective displacement due to foundation rocking is 0.14m. This corresponds to 51% of the maximum total displacement and is nearly 9 times larger than the response derived without taking foundation uplift into consideration. The maximum deck displacement due to the plastic hysteresis of the pier is 0.08m.

As shown in Fig. 5, the significant reduction of plastic deck displacement is a result of the reduced ductility demand at the base of the pier from 13.5 to 5.7 when foundation uplift is modelled in the analysis. This proves the significant isolation effect of foundation rocking.

Fig. 6 shows how large uplifts occur from the underlying ground at the left and right edge of the footing. The maximum uplifts along the longitudinal dimension of the footing are also presented here. The peak uplifts are 0.085m and 0.074m at the left and right edge, respectively.

Fig. 7 presents the subgrade reaction response under the corners of the footing. Maximum reactions along the footing in the longitudinal direction are also presented. The peak reactions are 1.75MPa and 1.95MPa at the left and right edge respectively. Since the capacity of the gravels is about 6MPa, the gravels do not yield.

It is important to note that contacts of the footing with the underlaid ground after separations result in large acceleration pulses, as shown in Fig. 8(a). The maximum peak vertical acceleration is 43.2m/sec^2 and takes place at the right corner of the footing. It is required to protect the ground under the footing not to suffer damage due to cyclic contacts and separations. The vertical accelerations cause significant variations of the axial load of the pier, as shown in Fig. 8(b).

Fig. 9 presents the moment vs. rotation hysteresis of the rocking response of the footing. Responses with and without modelling foundation uplifts are shown here. When uplifts of the foundation are disregarded, rocking response is linear elastic. On the other hand, hysteretic behaviour of the rocking response is complex when separations of the footing from the underlying soil are taken into account.

5. Response of the Bridge under Biaxial Excitation

Fig. 10 shows the seismic response of the bridge subjected to the NS component of JMA Kobe observatory record in the longitudinal direction and to the EW component of the same record in the transversal direction. The maximum total displacement of the deck is 0.27m. This is the same with the respective response under uniaxial excitation when foundation uplift is taken into account. However, under biaxial excitation, the maximum deck displacement due to foundation rocking is 0.22m which is approximately 80% of the total deck displacement. It is reminded that the same displacement under uniaxial excitation is 51% of the total deck displacement. This means that foundation rocking is more significant under biaxial excitation.

On the other hand, the maximum displacement of the deck due to inelastic behaviour of the pier is 0.02m, which is 25% of the respective response under uniaxial excitation. This fact is an immediate result of the reduced ductility demand at the base of the pier. As shown in Fig. 10(d), curvature ductility demand at the base of the pier in the longitudinal direction is 2, which is 38% of the respective response under uniaxial excitation when foundation uplift is also taken into account and 16% of the respective response under uniaxial excitation when foundation uplift is not taken into account. It is clear that the isolation effect of foundation rocking increases under biaxial excitation with respect to uniaxial excitation.

Fig. 11 shows the area of the footing which uplifts under uniaxial and biaxial excitation as a percentage of the total footing area. The uplifted area is significantly larger under biaxial excitation. As a mean value, 28.8% of the total footing area uplifts between $t=3.8\text{sec}$ and $t=20.3\text{sec}$ under uniaxial excitation while 46.3% under biaxial

excitation. At an instance, almost 95% of the entire area of the footing uplifts under biaxial excitation. The respective value under uniaxial excitation is 85%. Jumping of the footing does not occur at any instance during the excitation. It is worth noting, that under uniaxial excitation the uplifted area time history from one peak goes back to zero and then to the next peak. This occurs because when the footing uplifts in one direction it has to go back to its initial equilibrium position in order to uplift in other direction. This is not the case under biaxial excitation.

Under biaxial excitation maximum footing uplifts and maximum soil reactions beneath the entire area of the footing have the shape presented in Fig. 12. The maximum uplift of the footing is 0.22m and takes place at one corner of the footing. This is approximately 2.6 times larger the respective response under uniaxial excitation. The maximum reaction of the soil is 5.75MPa and takes place again at a corner of the footing. This is almost 3 times larger than the respective reaction under uniaxial excitation. However, since the capacity of the gravels is about 6MPa yielding of the underlying soil still does not occur.

Finally, Fig. 13 compares the moment vs. rotation hysteresis of the rocking response of the footing in the longitudinal direction under uniaxial and biaxial excitation. It is shown that the moment capacity of the footing under biaxial excitation is always smaller or equal to the one under uniaxial excitation. This is the reason why the isolation effect of foundation rocking increases under biaxial excitation. Furthermore, it is clear that the overall system (footing + soil) becomes more flexible and develops significantly higher rotations under biaxial excitation.

6. Response of the Bridge under Tri-axial Excitation

Fig. 14 shows the response of the bridge when the vertical component in addition to the bilateral excitation is applied to the structure. The maximum total deck displacement is 0.26m, in which 0.22m is resulted from the respective displacement due to foundation rocking. This is the same with the response under biaxial excitation. Maximum displacement due to inelastic behaviour of the pier is 0.015m. This is slightly smaller than the response under biaxial excitation. The slight difference is a result of the slightly reduced ductility demand at the base of the pier. In particular, curvature ductility demand decreases from 2 to 1.8 under tri-axial excitation with respect to biaxial excitation. Consequently, in the specific example, the vertical component of the earthquake ground motion is less significant on the isolation effect caused by foundation rocking.

Generally, the vertical component of the earthquake ground motion results in variations of the axial force of the pier and consequently of the moment capacity of the footing. This is clear from Fig. 15 where a comparison of the rocking hysteresis of the footing is presented under biaxial and tri-axial excitation. However, in most cases, these

variations are not very high and they occur only during very short duration. Consequently, they do not influence significantly the response of the bridge.

Maximum footing uplift is 0.21m and maximum reaction of the soil underlying the footing is 5.7MPa. Both these values occur at the same corners of the footing and are almost equal to the respective responses under biaxial excitation. The maximum uplifted area of the footing is 93% of its total area. Again jumping of the footing does not occur.

7. Parametric Study

7.1. The size of the footing

To investigate the influence of the size of the footing on the isolation effect of foundation rocking three different square footings are analyzed: (1) 8m×8m (2) 9m×9m and (3) 10m×10m. The cross section and the geometry of the pier are kept the same and the bridge is subjected to the JMA Kobe Observatory excitation record.

As the size of the footing increases the structure becomes stiffer and foundation rocking decreases. This is clear in Fig. 16(a) that presents how maximum deck displacements due to foundation rocking decrease as the dimensions of the footing increase. In particular, maximum rocking displacements reduce from 0.21m, 0.24m and 0.25m to 0.14m, 0.21m and 0.21m under uniaxial, biaxial and tri-axial excitation respectively as the dimension of the square footing increases from 8m to 10m. For all footing sizes, when foundation uplift is neglected, maximum displacement due to foundation rocking is only 0.015m.

Fig. 16(b) shows that the curvature ductility demand at the base of the pier increases significantly as the size of the footing increases. More precisely, as the dimension of the footing increases from 8m to 10m the ductility demand increases from 2.5, 1 and 1.4 to 10, 6.1 and 6 under uniaxial, biaxial and tri-axial excitation respectively. This means that the isolation effect of foundation rocking reduces significantly as the size of the footing increases. In the same figure, the same ductility demands are shown when foundation uplift is neglected in the analysis. It is observed that, in the specific example, these ductility demands are almost independent of the size of the footing. It is worth noting that for all footing sizes isolation effect of foundation rocking increases under biaxial excitation and tri-axial excitation with respect to uniaxial excitation.

7.2. The yield strength of the soil

Until now, it has been assumed that the yield strength of the underlying soil is high enough (6MPa) and consequently yielding of the soil does not occur. When the yield

strength of the soil is lower, yielding occurs. The behaviour of the underlying soil is assumed here to be elastoplastic.

Fig. 17 shows the response of an individual corner spring when the bridge is subjected to the NS component of the Kobe observatory record along its longitudinal direction when the yield strength of the soil is assumed to be 0.5MPa. Fig. 17(a) represents the hysteresis loops (vertical displacement vs. vertical stress) of the spring. Furthermore, Fig. 17(b) shows the vertical displacement response of the specific spring. It is worth noting that significant permanent settlements are developed. In particular, the permanent settlement at the same corner of the footing increases from 1.7mm to 46mm as the yield strength of the soil decreases from 6MPa to 0.5MPa. Therefore, it is important for preventing large residual tilt of the footing not to impose vertical stress which is excessively larger than the yield strength of the underlying soil. Finally, Fig. 17(c) shows the vertical reaction response of the same spring. It is observed that after a certain instance the reaction of the spring remains constantly equal to zero. This is an immediate result of the residual settlements of the underlying ground mentioned above.

When yielding of the soil occurs the reaction of the soil is limited by its yield strength. In this way, as the yield strength of the soil decreases the moment capacity of the footing also decreases. This is clear from Fig. 18(a) which presents a comparison of the moment vs. rotation hysteresis of the rocking response of the footing when the yield strength of the soil is 0.5MPa and 6MPa. As the moment capacity of the footing decreases the moment that can be transferred to the base of the pier also decreases. Thus the curvature ductility demand at the base of the pier reduces. This is shown in Fig. 18(b) where the curvature ductility demands of the pier are presented when the bridge is subjected to uniaxial, biaxial and tri-axial excitation respectively and the yield strength of the soil takes values between 0.5MPa and 6MPa. Under uniaxial excitation, the ductility demand increases from 1 to 5.7 as the yield strength of the soil increases from 1MPa to 2MPa. Then, the demand remains stable since under this excitation pattern the maximum developed stress of the soil is not greater than 2MPa. Under biaxial and tri-axial excitation the pier remains elastic when the yield strength is smaller or equal to 4MPa. Then, the ductility demand increases and becomes equal to 2 and 1.8 respectively for yield strength of the soil equal to 6MPa.

7.3. The moment capacity of the pier in the transversal direction

In all previous analyses the moment capacity of the pier in the transversal direction of the bridge was high enough (109.6MNm) and as a result no yielding of the pier occurred in this direction. Though, if the moment capacity of the pier in the transversal direction was lower, yielding of the pier would occur and this would limit the maximum moment that could be transferred at the base of the footing in this direction. As a result, foundation rocking would decrease in the same direction and this would reduce the favorable influence of biaxial excitation on the isolation effect of foundation rocking. To investigate the influence of the moment capacity of the pier in the transversal direction on

the isolation effect of foundation rocking in the longitudinal direction of the bridge, several analyses are conducted where the moment capacity at the base of the pier in the longitudinal direction of the bridge is the same as in previous chapters (49.6MNm) but the respective moment capacity of the pier in the transversal direction obtains the following values:

$$M_y^{\text{trans}} = [20, 40, 60, 80, 100] \text{ MNm}$$

Fig. 19(a) shows how maximum displacements due to foundation rocking in the longitudinal direction of the bridge decrease as the moment capacity of the footing in the transversal direction decreases. In particular, maximum rocking displacements in the longitudinal direction of the bridge decrease from 0.22m to 0.16m when the moment capacity of the pier in the transversal direction decreases from 100MNm to 20MNm. It is worth noting, that when the moment capacity of the pier in the transversal direction is 20MNm maximum displacements due to foundation rocking tend to be the same under uniaxial and biaxial excitation.

Fig. 19(b) presents maximum curvature ductility demands at the base of the pier in the longitudinal direction of the bridge as a function of the moment capacity at the base of the pier in the transversal direction. It can be seen that as the moment capacity of the pier in the transversal direction of the bridge decreases, curvature ductility demands at the base of the pier in the longitudinal direction of the bridge increase. In fact, as the yield moment of the pier in the transversal direction of the bridge decreases from 100MNm to 20MNm, maximum curvature ductility demands at the base of the pier in the longitudinal direction of the bridge increase from 2 to 4.6. It is reminded that the respective demand under uniaxial excitation is 5.7. From the above, it can be concluded that the favorable influence of biaxial excitation on the isolation effect of foundation rocking in one direction may be limited by the moment capacity of the pier in the perpendicular direction.

7.4. The excitation pattern

In order to investigate the sensitivity of rocking isolation to the characteristics of the ground motion, the pier is subjected to three additional excitation patterns. The first additional excitation pattern involves the ground motions recorded at the 74 Sylmar station during the 1994 Northridge earthquake. The 52° component is applied to the longitudinal direction and the 142° component is applied to the transversal direction of the bridge. The second additional excitation patterns concerns the ground motion recorded at the TCU084 station during the 1999 Chi-Chi Taiwan earthquake. North component is applied to the longitudinal and west component to the transversal direction of the bridge. Finally, the third additional excitation pattern involves the ground motions recorded at the 279 Pacoima Dam station during the 1971 San Fernando earthquake. The 164° component is applied to the longitudinal direction and the 254° to the transversal direction of the bridge. For all ground motion patterns, the bridge pier is subjected to uniaxial, biaxial and tri-axial excitation.

Table 1 summarizes maximum total deck displacements in the longitudinal direction of the bridge under all excitation patterns and uniaxial, biaxial and tri-axial excitation.

For all excitation patterns, maximum displacements predicted by the different finite element models are similar.

Table 2 shows the respective maximum deck displacements due to foundation rocking. It is clear the rocking displacements are highly underestimated when foundation uplift is not taken into consideration. Furthermore, rocking displacements increase significantly under biaxial excitation with respect to uniaxial excitation when foundation uplift is considered. The vertical component of the earthquake does not influence importantly the results.

Table 3 presents maximum foundation uplifts under all excitation patterns and uniaxial, biaxial and tri-axial excitation. Again, maximum uplifts of the footing increase significantly under biaxial excitation with respect to uniaxial excitation. Maximum uplifts are less sensitive to the vertical component of the excitation.

Finally, Table 4 presents maximum curvature ductility demands at the base of the pier in the longitudinal direction of the bridge. In all cases, curvature demands decrease drastically when foundation uplift is taken into account. The same Table shows that biaxial excitation has in all cases a favorable influence on the isolation effect of foundation rocking. The magnitude of this influence depends on the characteristics of the ground motion. On the other hand, the vertical component of the earthquake does not alter significantly the predicted damage in the pier.

8. CONCLUSIONS

The seismic response of a 10m tall standard bridge which is supported by a direct foundation was clarified taking the inelastic rocking response of the footing into account. The following conclusions may be deduced based on the results presented herein.

1) The direct foundation which is designed according to the traditional static analysis and the working stress design may rock separating from the underlaid ground when the bridge is subjected to the near field ground motion recorded in the 1995 Kobe earthquake. Maximum uplift of a corner of the footing is in the range of 0.2m. Separations of the footing from the underlaid ground occur as wide as 95% of the total area of the footing. However, jumping of the footing does not occur during the excitation.

2) If separations of the footing from the underlaid ground due to rocking response occur, the plastic deformation of the column at the plastic hinge decreases as a result of the softening of the moment vs. rotation hysteresis of the footing. As a consequence, the inelastic rocking of the footing results in an isolation effect on the response of the bridge.

3) This isolation effect of the inelastic rocking of the spread foundations is amplified under biaxial excitation of the bridge with respect to uniaxial excitation. Displacements due to foundation rocking, foundation uplifts and underlying soil reactions increase significantly under biaxial excitation.

4) The favourable influence of biaxial excitation on the isolation effect of foundation rocking depends on the characteristics of the ground motion records. Thus, individual analyses are required in order to be taken into account in design.

5) The vertical component of the earthquake does not alter significantly the isolation effect of inelastic foundation rocking. This occurs also for deck displacements due to foundation rocking, footing uplifts and soil reactions.

6) As the size of the footing increases foundation rocking and uplift decreases. Furthermore, since the moment capacity of the footing increases, potential damage of the column also increases. Thus, as the size of the footing increases isolation effect of foundation rocking decreases.

7) When yielding of the underlying soil occurs, the reaction of the soil is limited by its yield strength. In this way, as the yield strength of the underlying soil reduces the moment that can be transferred to the base of the pier decreases and the isolation effect of inelastic rocking of the foundation increases. However, yielding of the soil results in settlement of the underlying ground, which, in turn, causes residual tilt of the footing.

REFERENCES

- Carr, A.J. [2001] "Ruaumoko 3D Users Manual" University of Canterbury, Christchurch, New Zealand
- Ciampoli, M. and Pinto, P. E. [1995] "Effects of Soil-Structure Interaction on Inelastic Seismic Response of Bridge Piers," *Journal of Structural Engineering, ASCE*, Vol. 121 (5), 806-814
- Clough, R. W. and Huckelbridge, A. A. [1977] "Earthquake Simulation Tests of a Three-Story Steel Frame with Columns Allowed to Uplift," Report No. UCB/EERC 77-22, Earthquake Engineering Research Center, University of California, Berkeley
- Cremer, C., Pecker, A. and Davenne, L. [2001] "Modelling of Nonlinear Dynamic Behaviour of a Shallow Strip Foundation with Macro-element," *Journal of Earthquake Engineering*, Vol. 6, No. 2, 175-211
- Housner, G. W. [1963] "The Behaviour of Inverted Pendulum Structures During Earthquakes," *Bulletin Seismological Society of America* 53: 404-417
- Ishiyama, Y. [1982] "Motion of Rigid Bodies and Criteria for Overturning by Earthquake Excitations," *Earthquake Engineering and Structural Dynamics*, Vol. 10, pp. 635-650,
- Japan Road Association [1996] "Design Specifications of Highway Bridges,"
- Kawashima, K. and Unjoh, S. [1989] "Rocking Response of a Rigid Foundation Subjected to Seismic Excitation," *Civil Engineering Journal*, Vol. 32 (10), 60-66 (in Japanese)
- Kawashima, K. and Unjoh, S [1991] "Overturning of Rigid Foundation Resting on Ground with Insufficient Yield Strength," *Civil Engineering Journal*, Vol. 33(3), 54-59 (in Japanese)
- Kawashima, K., Unjoh, S. and Mukai, H. [1994] "Inelastic Rocking of Direct Foundation During an Earthquake," *Civil Engineering Journal*, Vol. 36(7), 50-55 (in Japanese)
- Kawashima, K. and Hosoiri, K. [2003] "Rocking Response of Bridge Columns on Direct Foundations" Proc. Fib-Symposium, Concrete Structures in Seismic Region, Paper No. 118, CD-ROM, Athens, Greece
- Priestley, N. M. J., Evison, R. J. and Carr, A. J. [1978] "Seismic Response of Structures Free to Rock on their Foundations," *Bulletin of the New Zealand Society for Earthquake Engineering*, Vol. 11, No. 3, 141-150
- Priestley, N. M. J., Seible, F. and Calvi, G. M. [1996] "Seismic design and retrofit of bridges," John Wiley & Sons, 1996
- Psycharis, I. [1982] "Dynamic Behaviour of Rocking Structures Allowed to Uplift," PhD Dissertation, California Institute of Technology, 1982

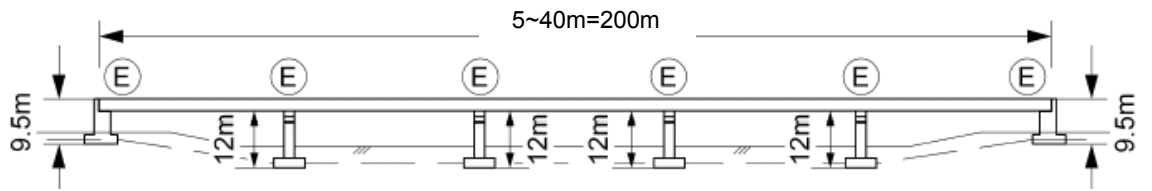


Fig. 1. Analyzed bridge

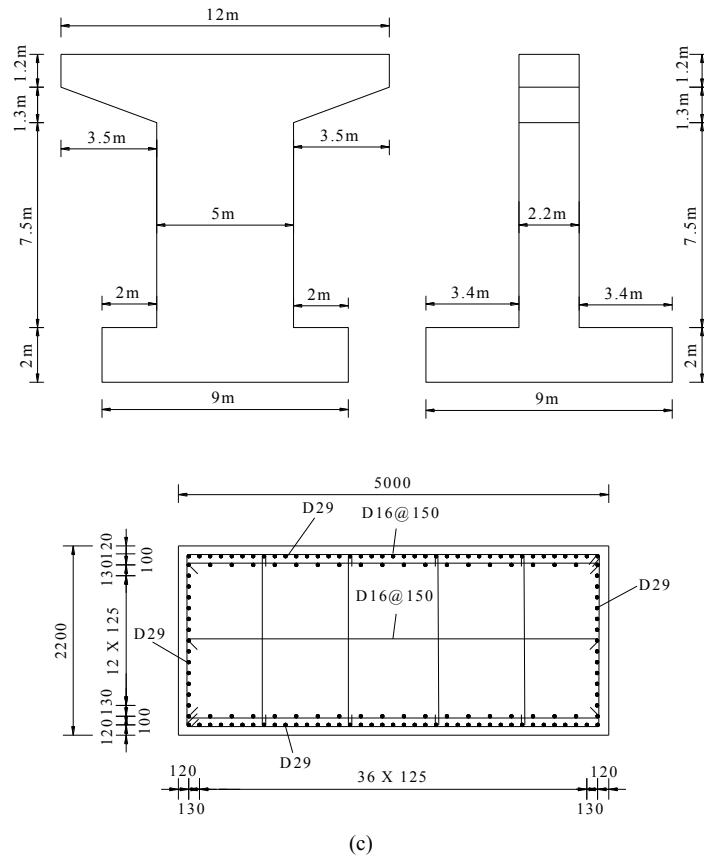


Fig. 2. Typical bridge pier: (a) front view; (b) side view; (c) cross section at the base of the pier

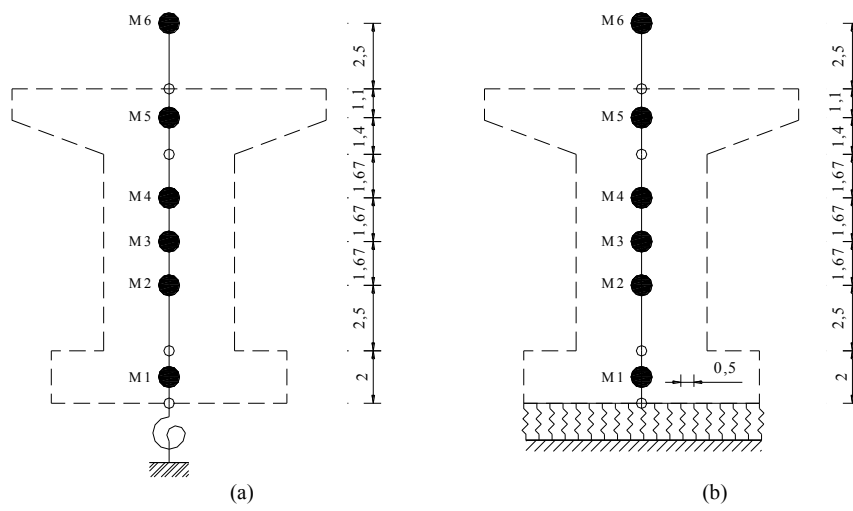


Fig. 3. Analytical models: (a) without modeling foundation uplift; (b) with modeling foundation uplift

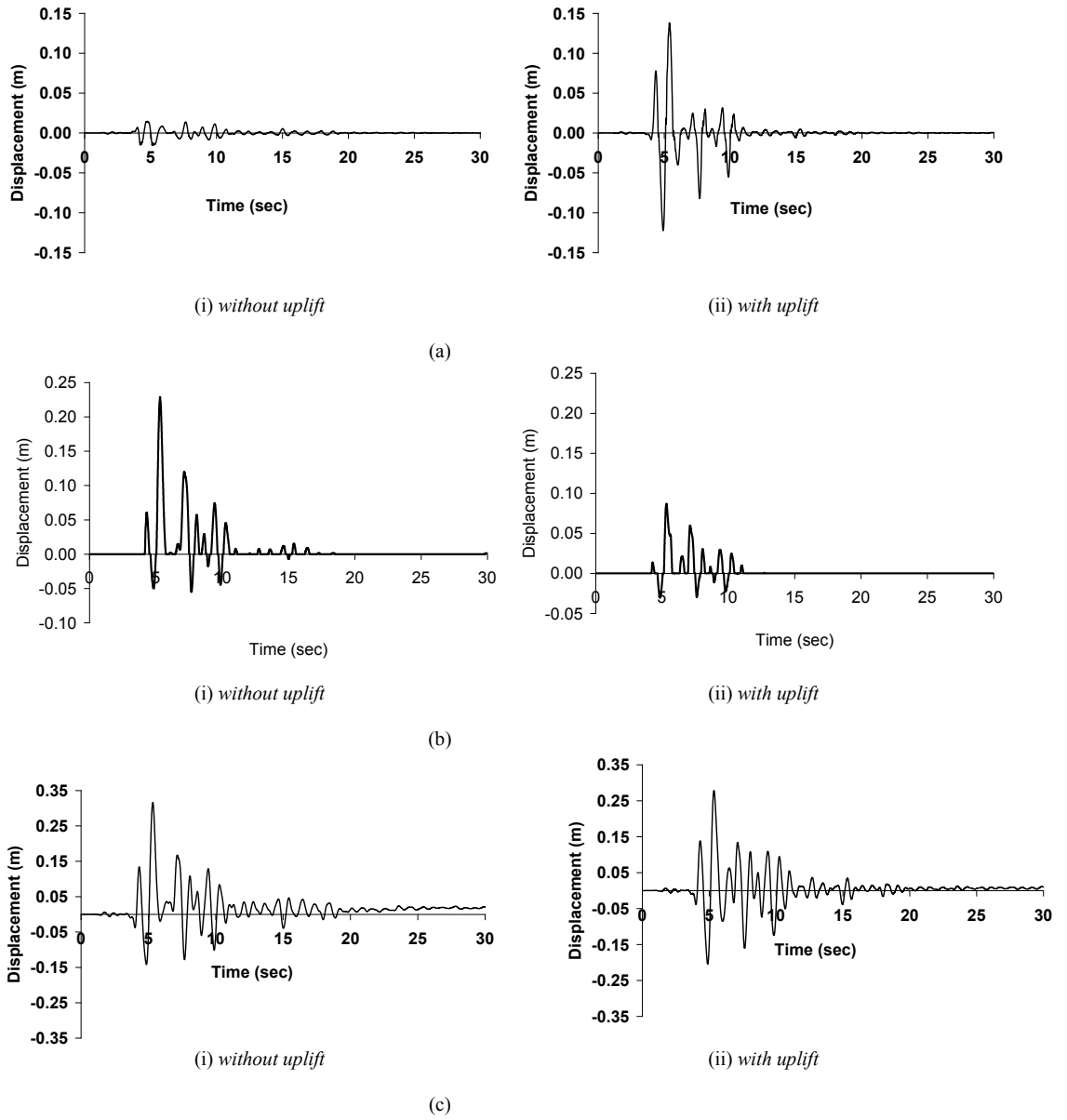


Fig. 4. Response of the bridge under uniaxial excitation: (a) displacements of the deck due to foundation rocking; (b) deck displacements due to inelastic behavior of the column; (c) total deck displacements

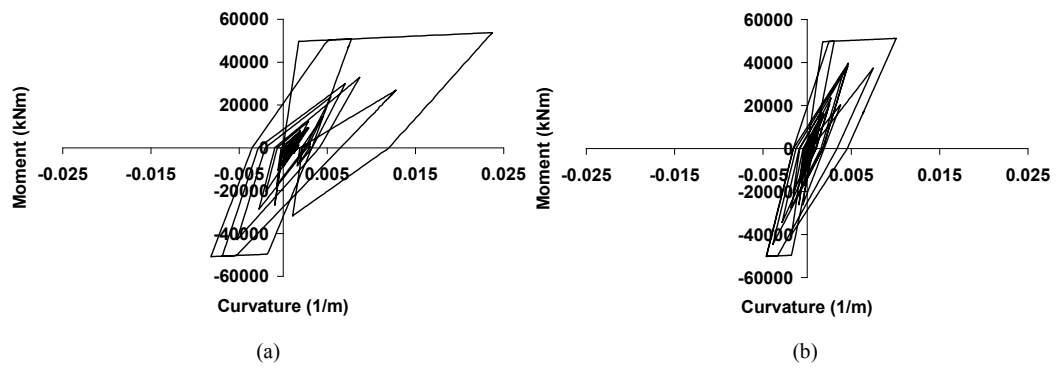


Fig. 5. Hysteresis loops at the base of the pier under uniaxial excitation: (a) without modeling foundation uplift; (b) with modeling foundation uplift

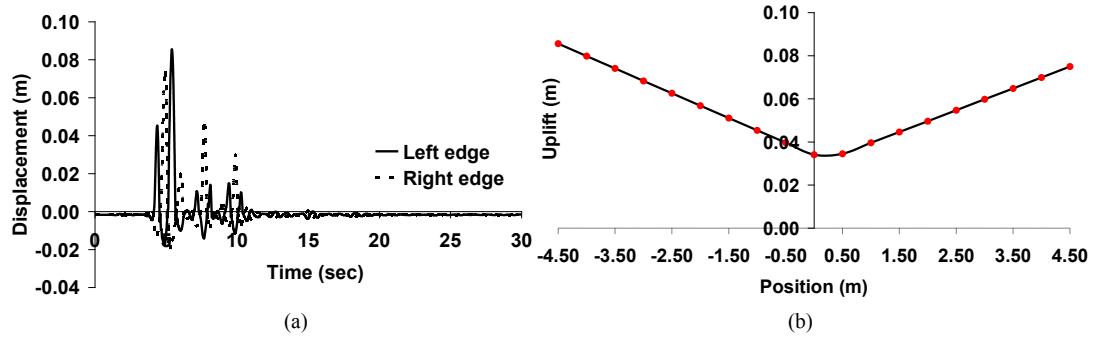


Fig. 6. Footing uplifts under uniaxial excitation: (a) uplift responses of the corners of the footing; (b) maximum uplifts along the footing in the longitudinal direction

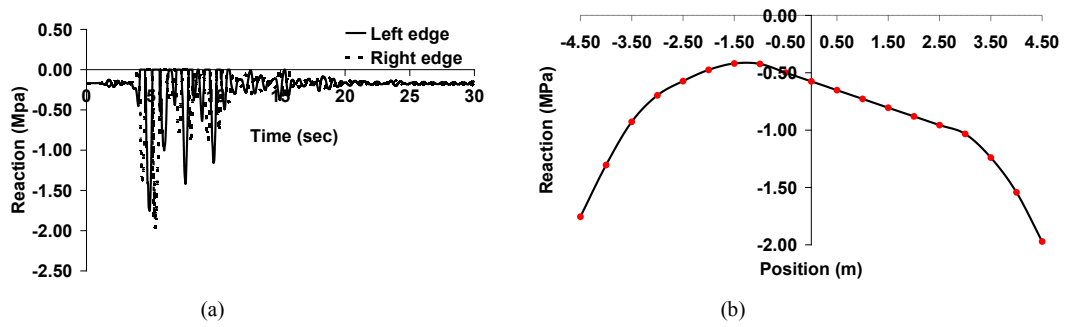


Fig. 7. Soil reactions under uniaxial excitation: (a) reaction responses under the corners of the footing; (b) maximum reactions along the footing in the longitudinal direction

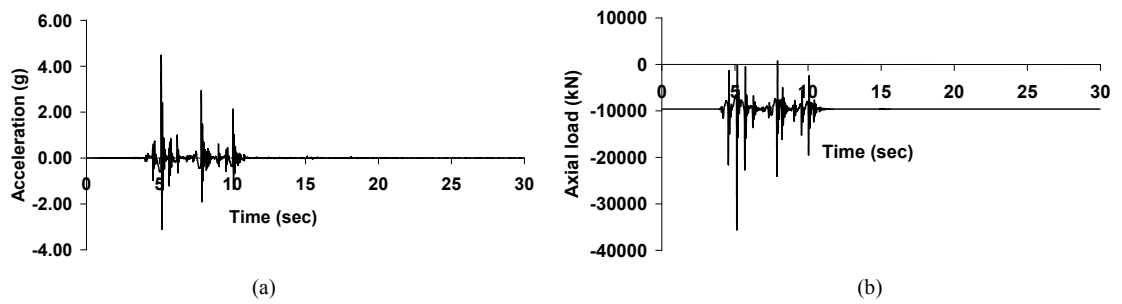


Fig. 8. (a) Vertical acceleration response at the right corner of the footing under uniaxial excitation; (b) axial force of the pier response under uniaxial excitation

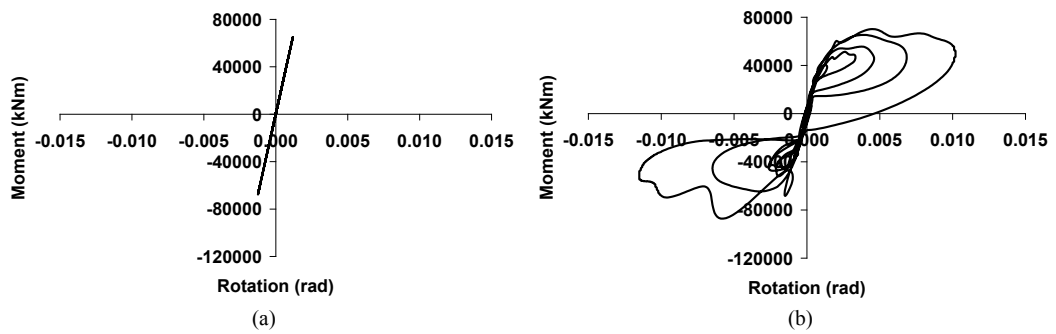


Fig. 9. Moment vs. rotation hysteresis of the rocking response of the pier under uniaxial excitation: (a) without modeling foundation uplift; (b) with modeling foundation uplift

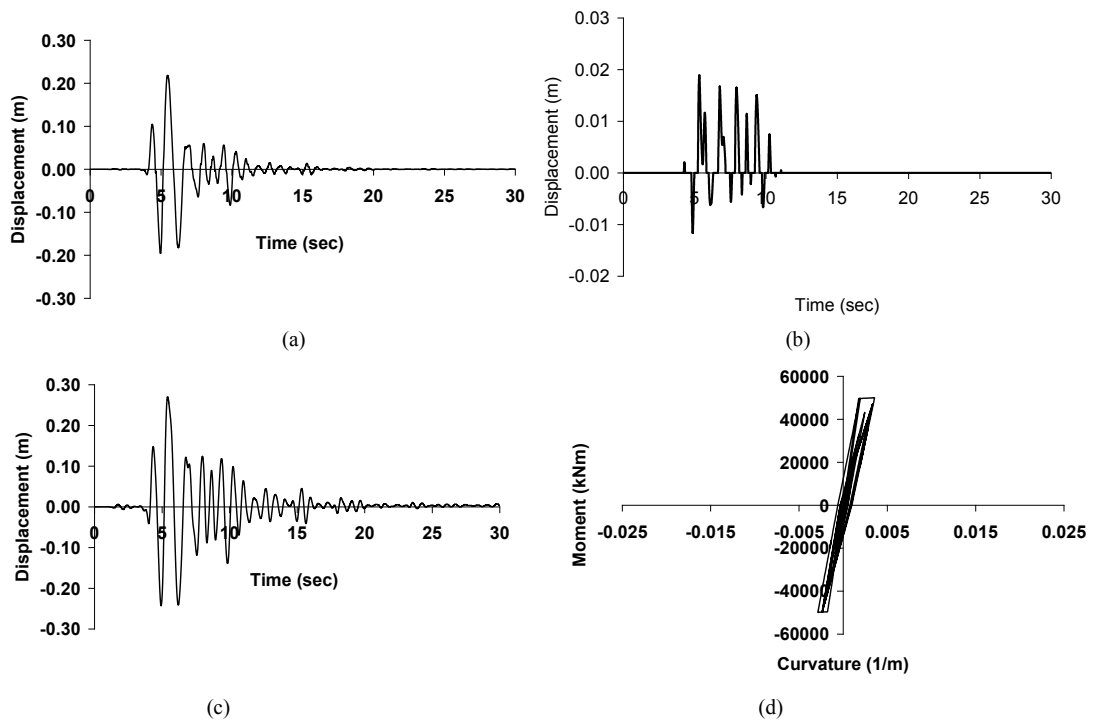


Fig. 10. Response of the bridge under biaxial excitation: (a) deck displacements due to foundation rocking; (b) deck displacements due to plastic behavior of the pier; (c) total deck displacements; (d) hysteresis loops at the base of the pier

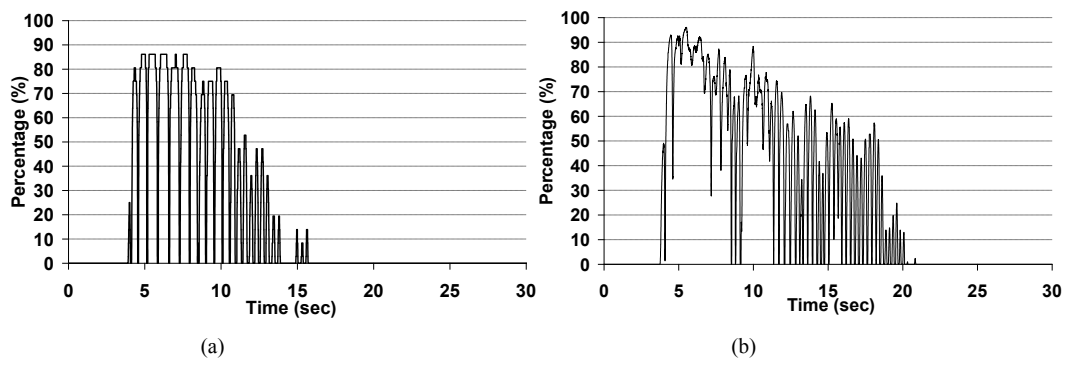


Fig. 11. Ratio (%) of the uplifted area over the total area of the footing: (a) uniaxial excitation; (b) biaxial excitation

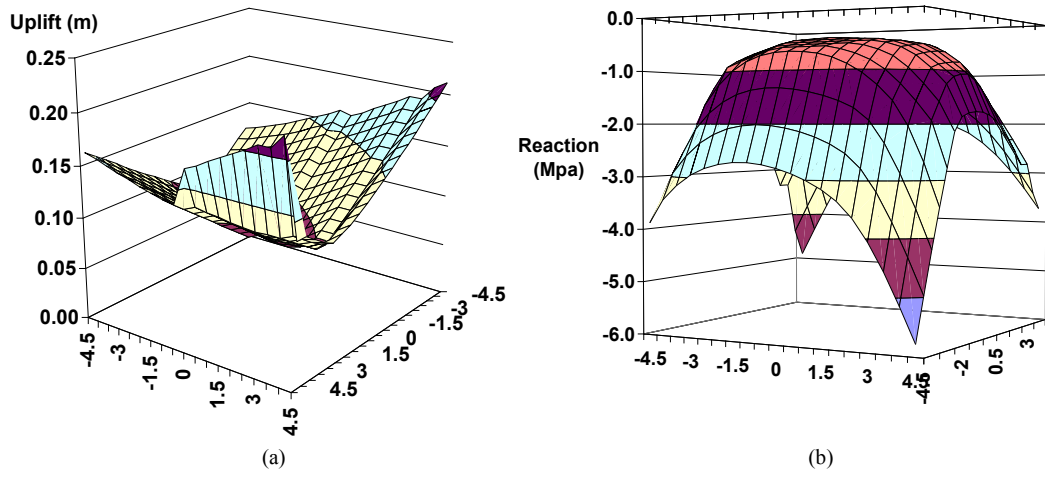


Fig. 12. (a) Maximum footing uplifts and (b) maximum reactions below the area of the footing under biaxial excitation

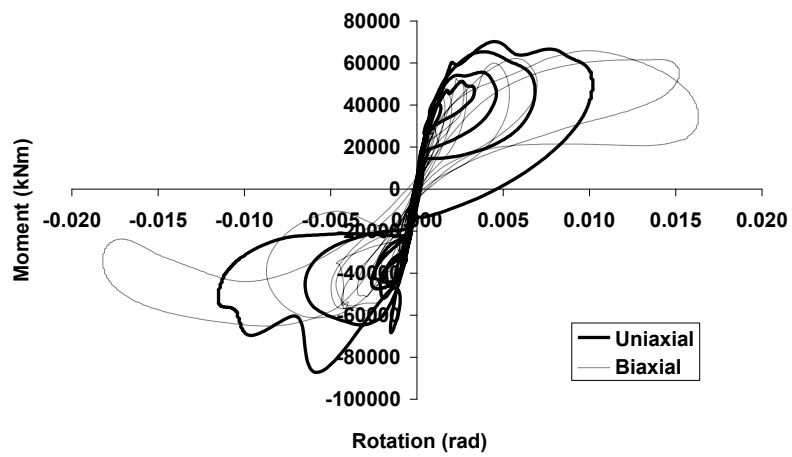


Fig. 13. Comparison of the moment vs. rotation hysteresis of the rocking response of the footing in the longitudinal direction under uniaxial and biaxial excitation

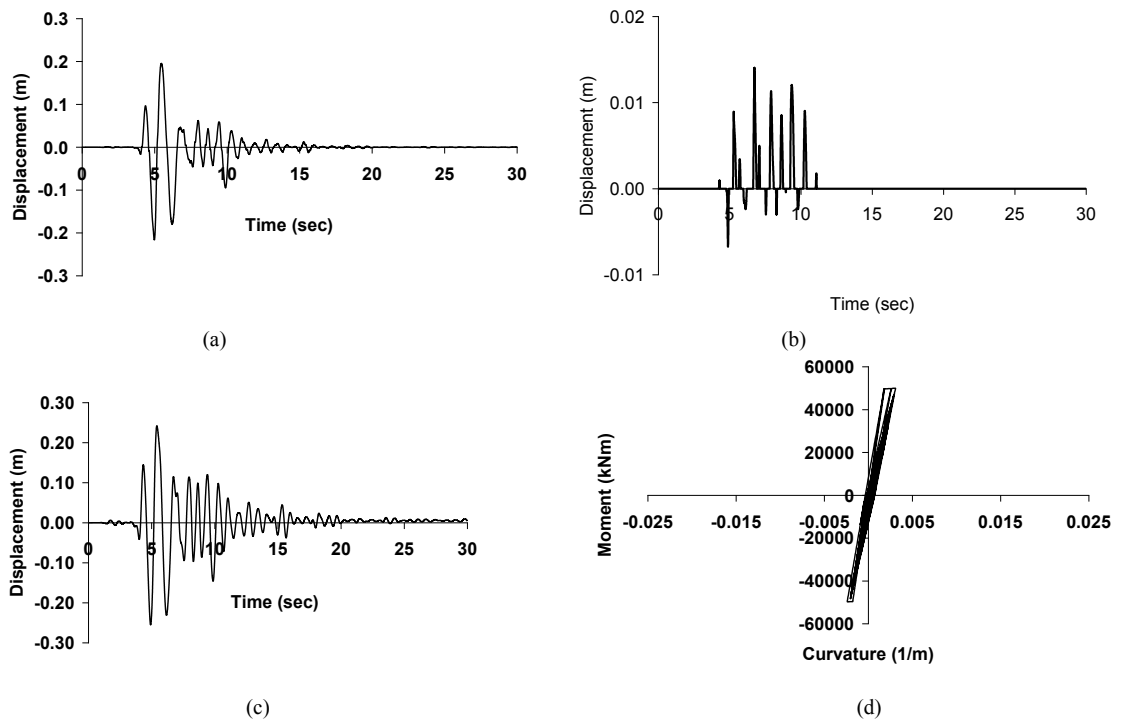


Fig. 14. Response of the bridge under tri-axial excitation: (a) deck displacements due to foundation rocking; (b) deck displacements due to plastic behavior of the pier; (c) total deck displacements; (d) hysteresis loops at the base of the pier

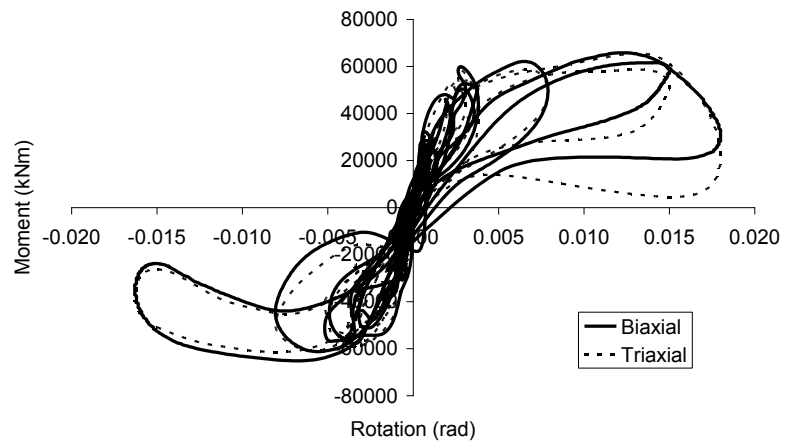


Fig. 15. Comparison of the moment vs. rotation hysteresis of the rocking response of the footing in the longitudinal direction under biaxial and tri-axial excitation

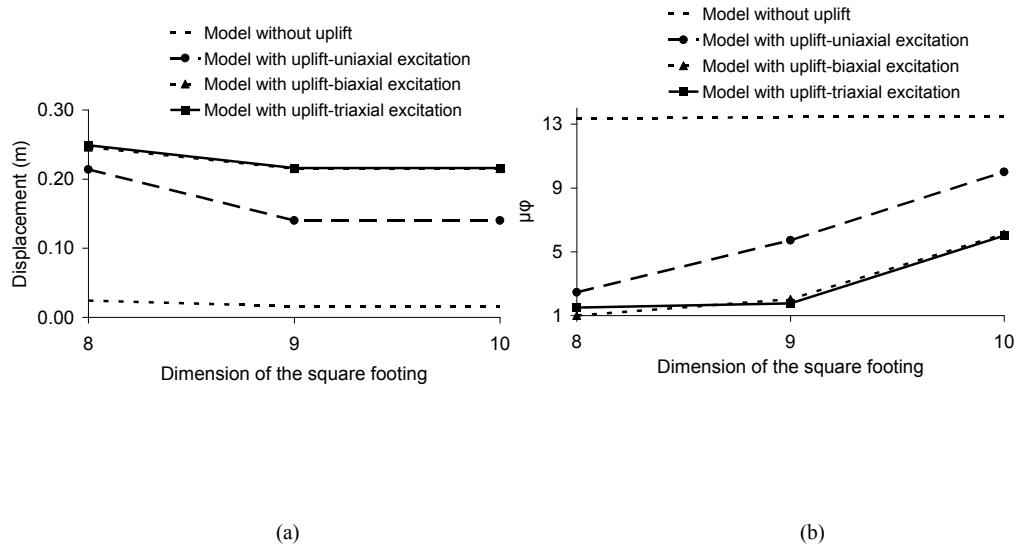


Fig. 16. Influence of the size of the footing on the response of the bridge: (a) maximum deck displacements due to foundation rocking; (b) maximum curvature ductility demands at the base of the pier

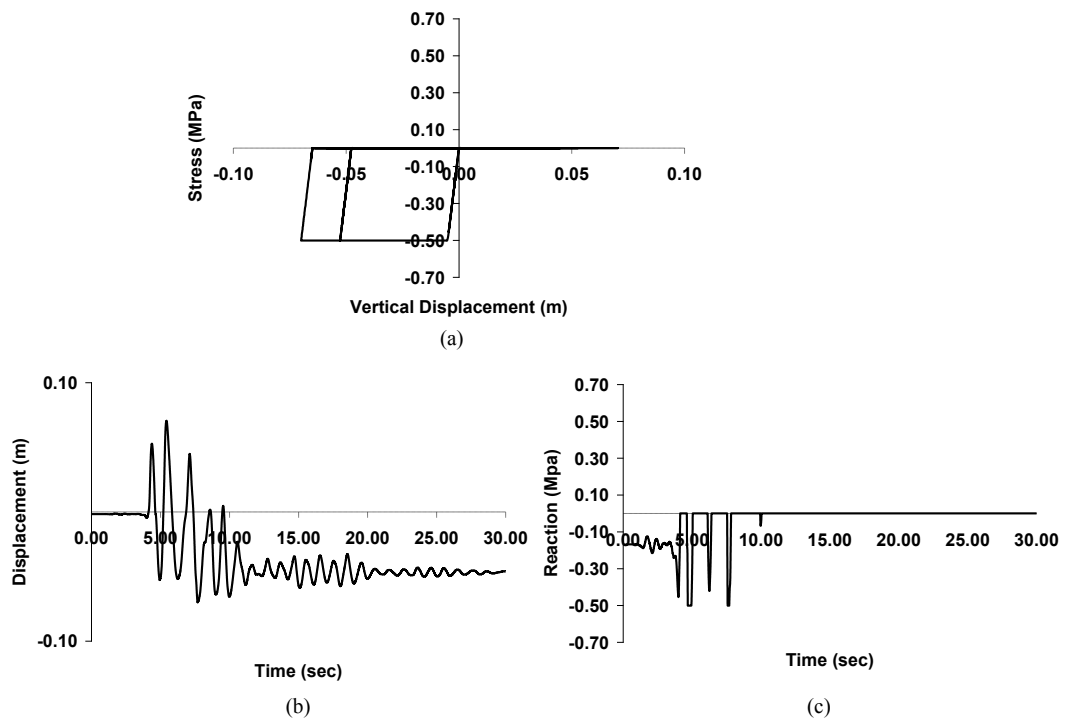


Fig. 17. Response of a corner spring having yield strength equal to 0.5MPa: (a) stress vs. vertical displacement hysteresis; (b) vertical displacement response; (c) vertical reaction response

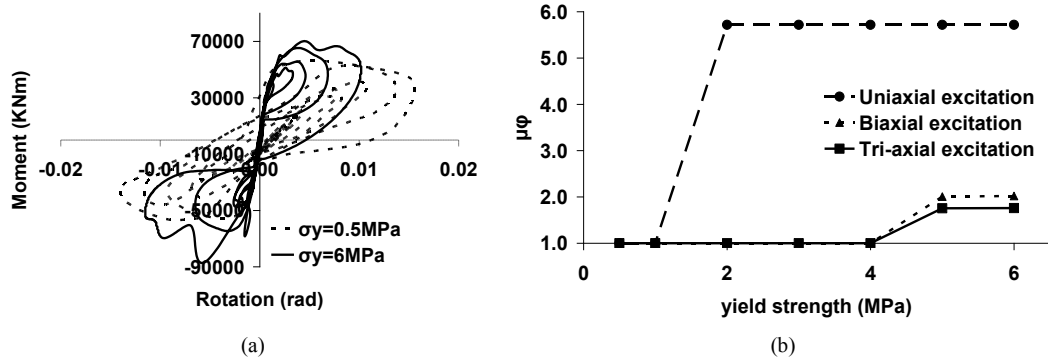


Fig. 18. Influence of the yield strength of the soil on the isolation effect of foundation rocking: (a) moment vs. rotation hysteresis of the rocking response of the footing when the yield strength of the soil is equal to 0.5MPa and 6MPa; (b) maximum curvature ductility demands at the base of the pier under uniaxial, biaxial and tri-axial excitation when the yield strength of the soil takes values between 0.5MPa and 6MPa.

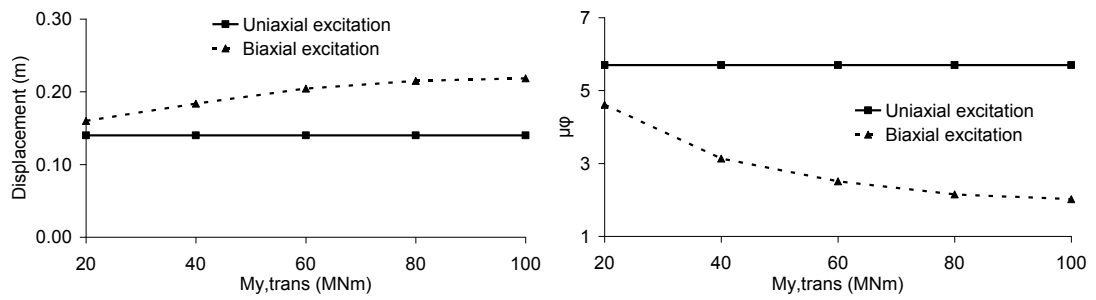


Fig. 19. Influence of the moment capacity at the base of the footing in the transversal direction of the bridge on the isolation effect of foundation rocking in the longitudinal direction of the bridge: (a) maximum deck displacements due to foundation rocking in the longitudinal direction of the bridge; (b) maximum curvature ductility demands at the base of the pier in the longitudinal direction of the bridge.

Table 1: Maximum total longitudinal deck displacements in meters for different excitation patterns				
Model/Earthquake	Kobe	Chi-Chi Taiwan	Northridge	San Fernando
Model without uplift	0.32	0.10	0.18	0.19
Model with uplift- Uniaxial excitation	0.27	0.11	0.17	0.20
Model with uplift- Biaxial excitation	0.27	0.13	0.21	0.21
Model with uplift- Tri-axial excitation	0.26	0.12	0.21	0.23

Table 2: Maximum longitudinal deck displacements due to foundation rocking in meters for different excitation patterns				
Model/Earthquake	Kobe	Chi-Chi Taiwan	Northridge	San Fernando
Model without uplift	0.02	0.01	0.02	0.02
Model with uplift- Uniaxial excitation	0.14	0.07	0.09	0.10
Model with uplift- Biaxial excitation	0.22	0.10	0.16	0.14
Model with uplift- Tri-axial excitation	0.22	0.09	0.16	0.16

Table 3: Maximum footing uplifts in meters for different excitation patterns				
Model/Earthquake	Kobe	Chi-Chi Taiwan	Northridge	San Fernando
Model without uplift	-	-	-	-
Model with uplift- Uniaxial excitation	0.09	0.04	0.06	0.06
Model with uplift- Biaxial excitation	0.22	0.16	0.16	0.11
Model with uplift- Tri-axial excitation	0.21	0.17	0.16	0.12

Table 4: Maximum curvature ductility demands at the base of the pier in the longitudinal direction of the bridge for different excitation patterns				
Model/Earthquake	Kobe	Chi-Chi Taiwan	Northridge	San Fernando
Model without uplift	13.5	2.8	6.8	5.0
Model with uplift- Uniaxial excitation	5.7	1.6	2.6	2.9
Model with uplift- Biaxial excitation	2.0	1.1	1.4	2.4
Model with uplift- Tri-axial excitation	1.8	1.1	1.1	2.5